

ATOMIC OXYGEN EFFECTS ON LDEF EXPERIMENT AO171

Ann F. Whitaker
Rachel R. Kamenetzky
Miria M. Finckenor
Joseph K. Norwood
NASA Marshall Space Flight Center
MSFC, AL 35812
Phone: 205/544-2510, Fax: 205/544-0212

INTRODUCTION

The Solar Array Materials Passive LDEF Experiment (SAMPLE), AO171, contained in total approximately 100 materials and materials processes with a 300 specimen complement. With the exception of experiment solar cell and solar cell modules, all test specimens were weighed before flight, thus allowing an accurate determination of mass loss as a result of space exposure. Since almost all of the test specimens were thermal vacuum baked before flight, the mass loss sustained can be attributed principally to atomic oxygen attack. This paper documents the atomic oxygen effects observed and measured in five classes of materials. The atomic oxygen reactivity values generated for these materials are compared to those values derived for the same materials from exposures on short term shuttle flights. An assessment of the utility of predicting long term atomic oxygen effects from short term exposures is given.

This experiment was located on Row 8 position A which allowed all experiment materials to be exposed to an atomic oxygen fluence of 6.93×10^{21} atoms/cm² as a result of being positioned 38 degrees off the RAM direction.

Composites

Table I summarizes the atomic oxygen erosion data for three carbon fiber and one glass fiber composite systems. A comparison of flight and control carbon fiber composites, figure 1, shows a darker, more diffuse surface as a result of flight exposure. Profilometer traces across the protected area of the bolt hole attachment points onto the exposed region of the flight specimen, figure 2, were used to generate thickness loss. Fiber bundles were easily discernible in the patterns of the traces. On a microscopic level, peak type structures characteristic of orbital atomic oxygen attack and "ash" material are observable on the exposed surfaces as is a protected "mesa" area, figure 3. Thickness losses measured on the flight specimens were consistent with their measured mass loss. Composite matrix erosion was greater than that of the carbon fibers and was most pronounced for the polysulfone P1700 system. Atomic oxygen reactivity values generally averaged 1×10^{-24} cm³/atom with the exception of the "S" glass epoxy composites which tend to become self protecting. Reactivity values generated from short term shuttle exposures yield twice the LDEF values noted here. A reasonable explanation is that high fluences accumulated through long

exposures readily erode the as-prepared matrix rich composite surfaces so that the fiber rich bulk region receives comparatively higher exposure. Reactivity values for high fluence exposed or long term exposed composites are thus more characteristic of the carbon fiber than the more reactive matrix material. As a result, long term prediction of erosion of carbon fiber composites should be based on carbon reactivity to give a more realistic measure of material loss. Short term exposures will yield erosion rates much too high for these materials.

Table I. AO171 Composites - Atomic Oxygen Erosion Rates

Composite Materials (No. of Specimens)	Avg. Thickness Loss (mils)	Atomic Oxygen Reactivity 10^{-24} cm^3/atom	Comments
* HMF 322/P1700/+/- 45°(5)	2.5 to 6.2*	0.92 to 2.3	On AO171: Matls. (1-5) "blackier, i.e. more diffuse. "S" glass epoxy much darker probably from UV effects. Fibers evident in materials (1-6). Material (7) shows unexplained corrugated features on Al tape. Shuttle Flights: Graphite/epoxy reactivity 2 to $2.6 \times 10^{-24} \text{ cm}^3/\text{atom}$
* HMS/934/0° (5)	2.5**	0.920	
* HMS/934/90° (6)	2.700	1.0	
* P75S/934/90° (6)	2.700	1.0	
* P75S/934/0° (5)	2.800	1.0	
* "S" Glass-epoxy (3)	0.36***	0.130	
* Thermal Control * Aluminized Taped "S" Glass-epoxy (3)	Indeterminate	---	

* Matrix erosion much greater than fiber

** Average of rates from 2 ends of sample; contamination likely on forward end

*** Fibers uneroded and become protective after initial matrix mass loss

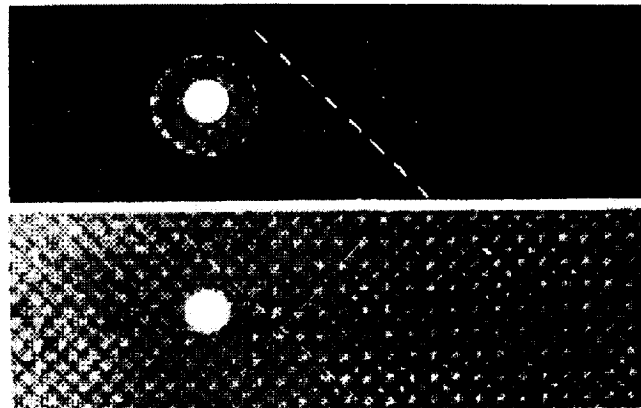


Figure 1. AO171 Carbon fiber composite flight (top) and control (bottom) specimens.

Paints

Table II contains absorptivity data and mass loss data for eight paints flown on LDEF compared with similar data obtained from short term shuttle flights. Control values of absorptivity were generated either on the sample flown or on control samples in the batch from

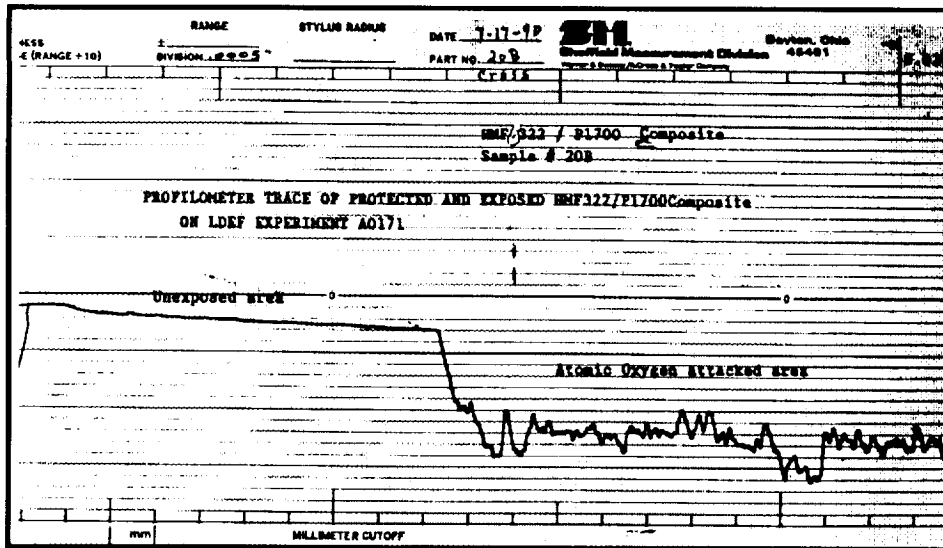


Figure 2. AO171 Carbon fiber profilometer trace.

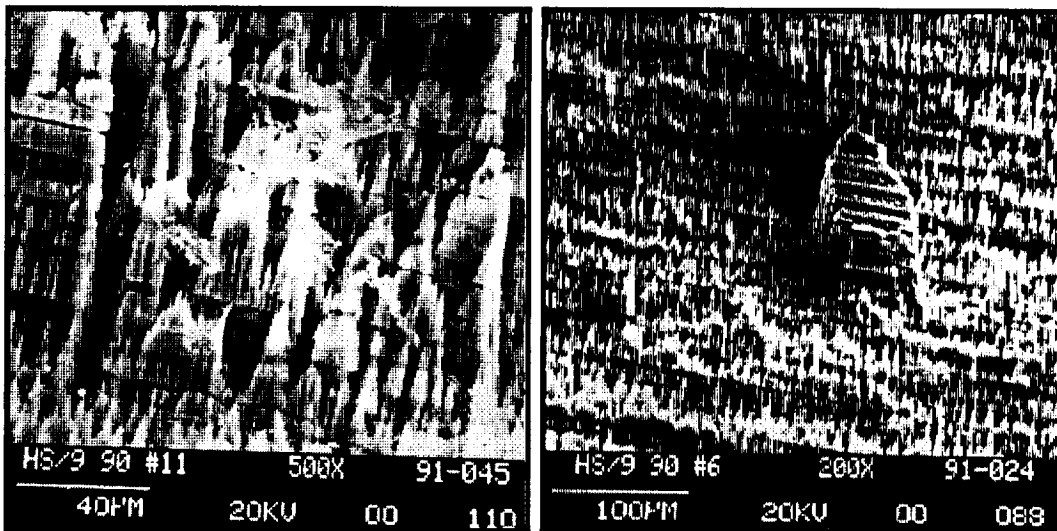


Figure 3. SEM photos of exposed carbon fiber composites showing peak type surface structure and "ash" material at 500x (left) and a protected "mesa" on the exposed surface at 200x (right).

which the flight samples were taken. With the exception of the Z302 black, all the paints that flew were optically diffuse. The trend for paints which do not drastically change color is to decrease in solar absorptivity, α_s , as a result of long term orbital atomic oxygen exposure whereas an increase in α_s is observed after similar short exposures. Under these short exposures to atomic oxygen, the surfaces of these diffuse paints increase in diffuseness but also have an accompanying increase in α_s . With long exposures in this environment, the colorless or lighter colored paint pigments are

Table II. Comparison of AO171 Flight Experiment and Shuttle Short Term Shuttle Paint Property Data

Paints	α_s Control	$\Delta\alpha_s$		Reactivity (mg/atom)	
		LDEF AO171	Shuttle Flight	LDEF AO171	Shuttle Flight
Z306 Black Diffuse	0.990	-0.010	-0.020	2.3×10^{-22}	1.0×10^{-21}
Z302 Black Specular	0.97 - 0.99	~ 0	0.040	5.7×10^{-22}	5.8×10^{-21}
Z853 Yellow Diffuse	0.41 - 0.49	-0.070	0.040	1.4×10^{-22}	0.90×10^{-21}
A276 White Diffuse	0.24 - 0.28	-0.050	~ 0	1.4×10^{-22}	1.0×10^{-21}
401-C10 Black Diffuse	0.98 - 0.99	3.7 ± 1.0	1.5 ± 0.5	1.6×10^{-22}	0.86×10^{-21}
Tiodized K17 White	0.38	0.030	Unavailable	Unavailable	No Data
Tiodized K17 Black	0.96	-0.15	Unavailable	Unavailable	No Data
S13GLO Diffuse White	0.19	0.14	1.1 ± 2	Negligible	Negligible

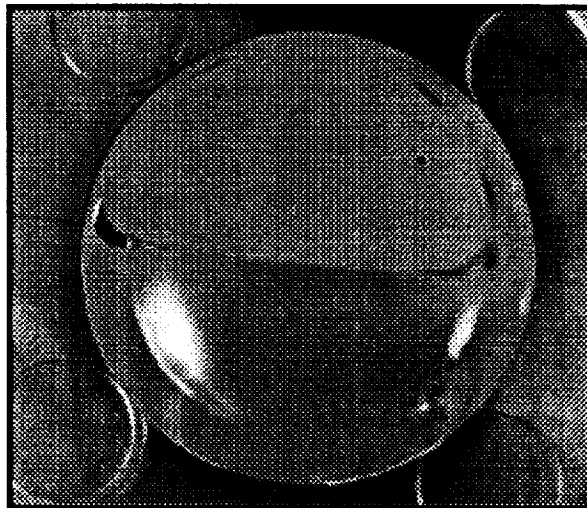


Figure 4. Post-flight photo of Z853 paint specimen shows a distinct contrast between the protected sample area and the lighter color exposed sample region.

exposed and have a greater influence on optical properties providing some increased reflectivity and a corresponding decrease in α_s . This increase in the reflectivity is observable in the Z853 yellow paint, figure 4, where the exposed area is lighter in color. Coincidentally, this specimen has sustained a micrometeoroid impact in the exposed area. The changes in optical properties for the

Tiodized paints are accounted for by the fact that the samples have lost their characteristic colors. The S13GLO white paint, which resisted atomic oxygen attack but darkened with exposure, doubled in absorptivity due probably from ultraviolet irradiation.

All the paints except S13GLO lost mass as a result of atomic oxygen exposure. The reactivity values for short and long term exposures are given in terms of milligrams per incident atomic oxygen atom rather than the conventional reactivity unit. These paints are diffuse implying the presence of inert components which do not erode, so thickness loss is not as sensitive a measure of atomic oxygen reactivity as is mass loss. As expected, the short term and long term reactivities are nonlinear so long term reactivities cannot be predicted from short exposures. With increased exposures more inert material is exposed, thus providing increased self shielding which results in

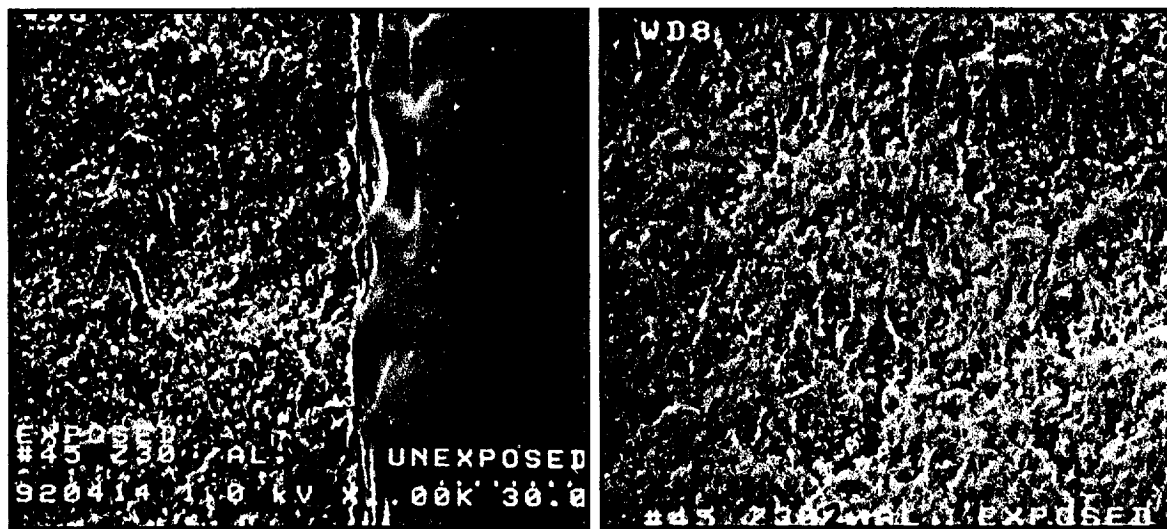


Figure 5. Micrographs of Z302 black paint showing the exposed/protected interface (left) and the "ash" material (right).

apparent decreased reaction to incident atomic oxygen. The benefit derived is that the paint will survive longer than predicted from short exposures. An eroded and controlled area on Z302 black is shown in figure 5 as is a microphotograph of the "ash" material which characteristically appears on orbital atomic oxygen exposed materials that contain black carbon.

Polymers

Polymers from Experiment AO171 whose reactivity values have been calculated from thickness decreases or mass loss are contained in table III with similar data generated from short shuttle exposures. These polymers consisted of thin films of white Tedlar, TFE Teflon washers, Polysulfone contained in carbon fiber composites and bulk samples of Halar, PEEK and RTV-511 and Kevlar 29 and 49 in woven fabrics. Mass loss due to atomic oxygen erosion in RTV-511 could

not be separated from vacuum outgassing so no reactivity value was generated for that material. Thin films of 5 mil Kapton, 1 mil black Kapton and 0.5 mil FEP Teflon were eroded away as a result of the 5.8 years of exposure.

White Tedlar contains self-shielding particles so that a residual film of Tedlar remained after exposure. These particles served to prevent a linear erosion of Tedlar with atomic oxygen fluence. No short term erosion data were available for this material for comparison. Profilometer traces across exposed and protected areas were used to determine atomic oxygen erosion of 40 TFE Teflon washers in order to generate TFE reactivity. This data is compared in table III to FEP Teflon data from LDEF Experiment S0069. This comparative analysis shows a definitive atomic oxygen erosion difference between TFE and FEP Teflon which short term exposure data could not previously resolve.

Kevlar 29 and 49 reactivity values on AO171 were based on thickness measurements of woven fabrics, and Kevlar 29 data from shuttle flight STS-8 was based on mass loss sustained from a woven tether. These data show a distinct difference in the response between Kevlar 49 and 29. Variability of sample configuration and method of determination of reactivity in the short term

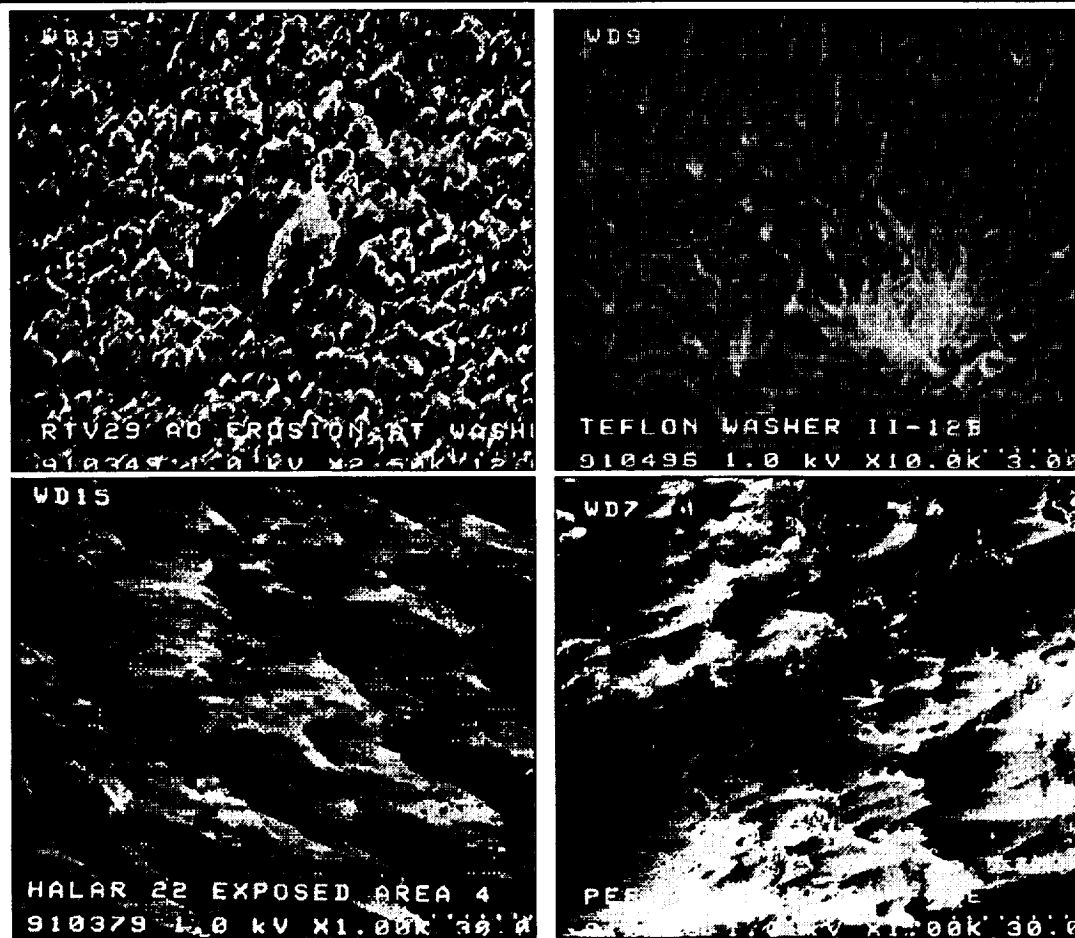


Figure 6. SEM photographs of AO171 exposed polymers (clockwise from top left) RTV 511, TFE Teflon, PEEK, and Halar.

STS-8 exposure and AO171 exposure for Kevlar 29 leave considerable uncertainty in the data. Kevlar 49 whose reactivity is higher is a more stressed material than is Kevlar 29, suggesting a connection between stress and atomic oxygen reactivity. Reactivity values for PEEK and Halar were derived from mass loss. Surface morphologies for selected exposed polymers from Experiment AO171 are shown in figure 6.

Atomic oxygen reactivity values for Experiment AO171 polymers are consistent with thermodynamic considerations and the effects of varying reactive constituents in materials. Polymers such as Polysulfone and Halar that represent pure polymers (i.e. polymers containing no components that erode at different rates) appear to erode linearly with atomic oxygen fluence, so long term thickness changes due to atomic oxygen attack in these materials can be predicted from short exposure data for these pure polymers.

Table III. Comparison of Atomic Oxygen Effects on Polymers from Experiment AO171 and Short Term Shuttle Flights

Polymer	Reactivity ($10^{-24}\text{cm}^3/\text{atom}$)		Comments
	AO171	Shuttle Flights	
White Tedlar	0.29	----	Inert particles retarded erosion
TFE Teflon	0.20	< 0.05 (estimated)	Data from SOO69
FEP Teflon	0.35	< 0.05 (estimated)	
PEEK	2.3	3.7 ± 1.0	Shuttle tested material was thin film with low emittance
Halar	2.1	2.0	Shuttle data based on STS-8 tether mass loss
Kevlar 29	1.5 ± 0.5	1.1 ± 2	
Kevlar 49	4.0	---	
Polysulfone	2.3	2.4	

Metals

The metals complement of experiment AO171 consisted of various copper and silver ribbon materials, miscellaneous metallic specimens, and 1" diameter bulk metals including materials which readily oxidize and which resist oxidation in the atomic oxygen environment. A series of alloys containing various ratios of aluminum, chromium and nickel in the as-received and preoxidized condition were also flown. Cold rolled silver ribbon both thermally heat sunk to the experiment base and thermally isolated configured with and without a stress loop completed the metal samples reported on here. Data generated from the analyses of these materials are contained in table IV.

Macroscopic oxidation effects were observed in silver and copper. The orbital oxidation effects observed in copper have not been previously reported, partly because the effect in copper was not anticipated. Some fine structure is observable on the flight exposed copper surface of figure 7. The microstructure for the different silver samples is shown in figure 8. The silver oxide scaling on the cold rolled ribbon has been seen previously but the fine grained oxide

structures from the disk samples have not been previously observed. Most of the metals flown on this experiment were not finely polished so the microphotographs show large features which are machine marks from the sample preparation process. The atomic oxygen effects in the other metals appear to be minimal. With the exception of some of the silver samples, the metals were well heat sunk to the less than 100°F experiment structure. It is well known that temperature plays a strong role in oxidation phenomena, and the low temperatures to which these heat sunk metals were subjected would not be expected to accelerate oxidation.

All the metals reported on gained weight as a result of being exposed to orbital atomic oxygen. Reactivity values based on linear effects were reported for these materials even though it is known that metals oxidize nonlinearly. This was done in order to give a comparative measure of the observed effects. With the exception of silver, the magnitude of reactivity numbers was less than $1 \times 10^{-26} \text{ cm}^3/\text{atom}$ for the conditions experienced on AO171. Accommodation numbers presented are given in terms of atomic oxygen atoms reacted ratioed to the incident atoms. These calculations based on the mass increase show that, with the exception of stressed, thermally isolated silver, less than 10 atoms per 10^4 incident are reacted. The basic assumption for these accommodation numbers is that the mass increase resulted from the formation of the most thermodynamically favorable oxide. The presence of some of these oxides is yet to be confirmed. The reactivity and accommodation values for the cold rolled, stressed, and thermally isolated silver are an order of magnitude greater than that of the same material which had no additionally applied stress and was heat sunk to the structure. These results suggest that the atomic oxygen effects are more dependent on temperature and microstructure than on total incident atomic oxygen.

Table IV. LDEF AO171 Metals Data

Metal	Reactivity ($10^{-26} \text{ cm}^3/\text{atom}$)	Accommodation of AO per 10^4 Incident Atoms	Comments
Copper	0.87	3.6	Accommodation strongly dependent on temperature and stress, numbers are tentative pending confirmation of oxide identity.
Molybdenum	0.14	2.8	
Tungsten	0.044	~ 1.0	
HOS 875	0.29	2.5	
Pre-Ox HOS 875	TBD	TBD	
Tophet 30	0.55	5.0	
Ni-Cr-Al-Zr Alloy	TBD	TBD	
Pre-Ox Ni-Cr-Al-Zr	---	---	
Tantalum	0.60	8.3	
Titanium 75A	0.39	4.4	
Mg AZ31B	0.45	2.0	
Niobium	0.14	2.0	
Silver disk-fine grain	2.9	8.4	
Silver - cold rolled ribbon in stress loop	27.5	80.0	



Figure 7. Microphotographs of LDEF AO171 copper sample protected surface (left) and exposed surface (right).

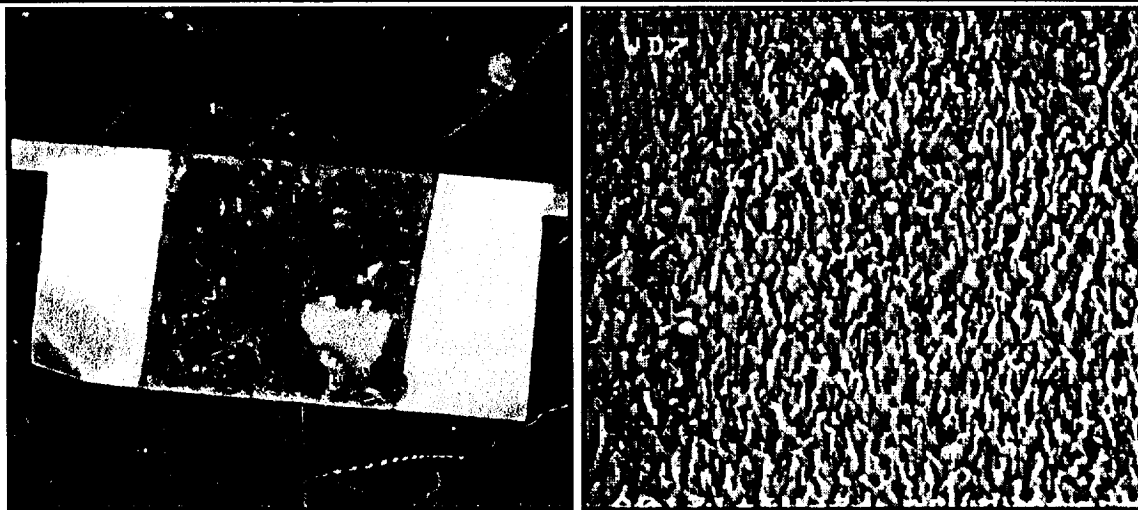


Figure 8. Photograph of LDEF AO171 silver interconnect (left) and SEM photograph of bulk silver exposed surface (right).

Glassy Ceramics

Approximately thirty silver and aluminum solar reflectors with thin coatings of various glassy ceramics were flown on this experiment. A large group of these reflector samples were configured with one-half of the sample exposed and the other half covered. Small decreases in reflectivity were noted in these samples but no contamination was present to account for these reflectivity decreases. Precision angstromer traces were made on all the samples, and it was noted

that a decrease in film height occurred in the exposed areas. Selected samples were examined with low energy Rutherford backscattering which revealed that a densification of the film materials had occurred in the exposed region. A conversion of SiO to SiO₂ was identified. The results of these measurements are presented here under atomic oxygen effects. However, several factors can bring about the densification of these materials and it remains to be proven that the effects noted are the result of atomic oxygen attack. Table V provides a listing of these effects for the various solar reflectors. Decreases in thickness of these materials range up to 160 angstroms. For applications of these materials where the total coating thickness is 1000 to 1300 angstroms, the percentage change is considerable and the effect can be substantial for space optics. Reactivity values for these materials are based on the assumption that the observed effects result from atomic oxygen attack range from 0.4 to 2.3 x 10⁻²⁸ cm³/atom.

Table V. Property Changes in AO171 Glassy Ceramics

Coating/Solar Reflector	Change in Solar Reflectance (%)	Decrease in Film Thickness (Å)	Comments
SiO ₂ / Ag	- < 1	40	No changes observed for <i>shuttle flight</i> exposures. On LDEF SiO-SiO ₂ , increase in film density noted. Defects observed on all reflectors except SiO ₂ /Al, small decreases in R _s measured. Reactivity ranges from 0.4 to 2.3 x 10 ⁻²⁸ cm ³ /atom for these materials.
SiO ₂ / Al	- < 1	50	
SiO-SiO ₂ / Enhanced Al	-2	125	
SiO / Al	-1.5	150	
MgF ₂ -Sapphire/Enhanced Al	+1.5	25	
MgF ₂ -Sapphire/Ag	-5 to -10	150	
Dielectric / Ag Alloy	-1 to -5	160	

SUMMARY

Table VI contains a summary of the atomic oxygen effects on five classes of materials exposed on LDEF experiment AO171. Unfilled polymers constitute the materials class in which long term erosion is predictable from short term exposures. The reaction of the remaining classes of materials appears to be considerably more complex so that prediction of long term effects must be based on factors other than thickness reduction.

Table VI. Summary of Long Term Atomic Oxygen Effects on AO171 Materials

Material	Atomic Oxygen Effects
Composites	Erosion from carbon fiber composites can be predicted from carbon reactivity. Glass fiber composites become self protecting.
Paints	Diffuse paints erode non-linearly.
Polymers	Unfilled polymers react linearly with atomic oxygen.
Metals	Reaction is non-linear and strongly dependent on temperature, stress and microstructure; accommodation on the order of less than 10 atoms per 10^4 incident.
Glassy Ceramics	Densification accompanied by a decrease of less than a few hundred angstroms results from space exposure.

Bibliography

1. Kamenetzky, R. R. and Whitaker, A. F., "Performance of Thermal Control Tape in the Protection of Composite Materials to Space Environmental Exposure", NASA TM-103582.
2. Whitaker, Ann F. and Young, Leighton E., "An Overview of the First Results on the Solar Array Passive LDEF Experiment (SAMPLE), AO171", First LDEF Post-Retrieval Symposium, Orlando, Fl., June, 1991.
3. Whitaker, Ann F., Finckenor, Miria M., and Kamenetzky, Rachel R., "Property Changes Induced by the Space Environment in Polymeric Materials on LDEF", AIAA 30th Aerospace Sciences Meeting, Reno, NV, January, 1992.
4. Whitaker, Ann F., "Selected Results for Metals from LDEF Experiment AO171", LDEF Materials Workshop '91", NASA/Langley Research Center, Hampton, Va., November, 1991.

